

Scheduling of Radiation with Angiogenesis Inhibitors Anginex and Avastin Improves Therapeutic Outcome via Vessel Normalization

Ruud P.M. Dings,¹ Melissa Loren,² Hanke Heun,¹ Elizabeth McNeil,³ Arjan W. Griffioen,⁴ Kevin H. Mayo,¹ and Robert J. Griffin⁵

Abstract Purpose: To test whether a direct antiangiogenic peptide (anginex) and a vascular endothelial growth factor antibody (bevacizumab, Avastin) can transiently normalize vasculature within tumors to improve oxygen delivery, alleviate hypoxia, and increase the effect of radiation therapy. **Experimental Design:** Tumor oxygenation levels, microvessel density and pericyte coverage were monitored in three different solid tumor models (xenograft human ovarian carcinoma MA148, murine melanoma B16F10, and murine breast carcinoma SCK) in mice. Multiple treatment schedules were tested in these models to assess the influence on the effect of radiation therapy. **Results:** In all three tumor models, we found that tumor oxygenation levels, monitored daily in real time, were increased during the first 4 days of treatment with both anginex and bevacizumab. From treatment day 5 onward, tumor oxygenation in treated mice decreased significantly to below that in control mice. This “tumor oxygenation window” occurred in all three tumor models varying in origin and growth rate. Moreover, during the treatment period, tumor microvessel density decreased and pericyte coverage of vessels increased, supporting the idea of vessel normalization. We also found that the transient modulation of tumor physiology caused by either antiangiogenic therapy improved the effect of radiation treatment. Tumor growth delay was enhanced when single dose or fractionated radiotherapy was initiated within the tumor oxygenation window as compared with other treatment schedules. **Conclusions:** The results are of immediate translational importance because the clinical benefits of bevacizumab therapy might be increased by more precise treatment scheduling to ensure radiation is given during periods of peak radiosensitivity. The oxygen elevation in tumors by non-growth factor-mediated peptide anginex suggests that vessel normalization might be a general phenomenon of agents directed at disrupting the tumor vasculature by a variety of mechanisms.

Angiogenesis is involved in various pathologic disorders like cancer, arthritis, diabetic retinopathy, and restenosis, but is also key to normal organ development (1). Agents that can inhibit angiogenesis in tumors have shown promise as therapeutics against cancer. Although anti-vascular endothelial growth factor (VEGF) agents like bevacizumab (Avastin, a humanized

monoclonal antibody against VEGF; Genentech) are perhaps most discussed (2), many other antiangiogenic compounds targeting some aspects of VEGF signaling have been identified and are currently in various phases of clinical cancer trials according to the National Cancer Institute clinical trials website. Nevertheless, some angiogenesis inhibitors are ineffective or cause unwanted biological side effects (3), which underscores the need for better angiostatic compounds and/or treatment strategies.

It is critical to recognize that antiangiogenesis treatment can take the form of more than VEGF pathway inhibition alone. Besides anti-VEGF compounds, which can be considered rather indirect angiogenesis inhibitors, one can categorize other inhibitors as direct antiangiogenesis compounds (i.e., affecting activated endothelial cells directly) or vascular disrupting agents (e.g., combretastatin) and others (e.g., arsenic trioxide, interleukin 8, interleukin 2, and tumor necrosis factor α ; ref. 4). Yet, currently, this is not reflected in clinical trials where predominantly VEGF inhibitors are being tested. At least in theory, the most promising angiogenesis inhibitors are those that act directly on endothelial cells to inhibit tumor angiogenesis, reducing the risk of drug resistance and making them more therapeutically effective against a broad spectrum of tumors (1). In clinical trials thus far, the addition of Avastin to standard chemotherapy has generally improved survival and

Authors' Affiliations: Departments of ¹Biochemistry, Molecular Biology, and Biophysics; ²Therapeutic Radiology-Radiation Oncology; and ³Veterinary Clinical Sciences, University of Minnesota, Minneapolis, Minnesota; ⁴Angiogenesis Laboratory, Research Institute for Growth and Development, Department of Pathology, Maastricht University and University Hospital, Maastricht, the Netherlands; and ⁵Department of Radiation Oncology, University of Arkansas for Medical Sciences, Little Rock, Arkansas

Received 10/6/06; revised 1/12/07; accepted 3/13/07.

Grant support: National Cancer Institute grant R01 CA-107160 (R.J. Griffin) and R01 CA096090 (K.H. Mayo), and grants from Dr. Saal van Zwanenberg Stichting and the Koningin Wilhelmina Fonds (H. Heun).

The costs of publication of this article were defrayed in part by the payment of page charges. This article must therefore be hereby marked *advertisement* in accordance with 18 U.S.C. Section 1734 solely to indicate this fact.

Requests for reprints: Robert J. Griffin, Department of Radiation Oncology, University of Arkansas for Medical Sciences, 4301 West Markham #824, Little Rock, AR 72223. Phone: 501-526-7873; Fax: 612-626-6245; E-mail: rjgriffin@uams.edu.

© 2007 American Association for Cancer Research.

doi:10.1158/1078-0432.CCR-06-2441

response rate by 10% to 15% and has been shown to cause clinically evaluable changes in tumor physiology (5, 6). However, not every combination study with Avastin has shown improved efficacy. Second- or third-line patients with metastatic breast cancer in a phase III trial did not benefit from the addition of bevacizumab to capecitabine (7). It is now generally accepted that tumors can evade the blockade of a single growth factor such as VEGF by relying more heavily on one or more of nearly a dozen other growth factors shown to be involved in angiogenesis and vascular homeostasis (8). Clearly, there is a need to diversify and investigate other angiogenesis mechanisms and targets and to optimize clinical translation of these exciting therapeutics in combination with radiation and chemotherapy.

Numerous preclinical studies have indicated that the addition of various types of antiangiogenic or antivascular therapy to single-dose or fractionated radiotherapy can synergistically improve the response of human and murine tumors to treatment (5, 9–13). However, because there are multiple variables that contribute to the sensitivity of tumors to radiation or antiangiogenic treatment, it has been difficult to clearly identify a method to combine these therapies (14–16). Some investigations revealed that blocking survival signaling in endothelial cells after irradiation is highly effective in increasing the radiation response (11, 17). Others indicate that sensitization and killing of endothelial cells just before exposure to radiation may be the most effective way to improve radiation response (12, 13, 18, 19). In any scenario of combination treatments, the effect of one therapy (such as induction of hypoxia via blood vessel damage) may be detrimental to another (such as hypoxic radioprotection or reduced access of chemotherapy to the tumor). A logical and clearly proven rationale for optimal multimodality therapy is a necessity for efficient translation of successful preclinical strategies to human clinical applications (14, 15).

The accepted dogma is that antiangiogenic therapy destroys or blocks the function of tumor-associated vessels to deprive the tumor of oxygen and nutrients, thereby inhibiting tumor growth. However, current thinking leads one to conclude that the results of any type of antiangiogenic therapy depend on the time of administration and assessment. Recently, Jain et al. showed that blocking VEGFR2 causes the destruction of “immature” vessels and thus improves the overall physiologic state of the tumor over a specific span of time (20, 21). For this effect, Jain et al. coined the phrase “normalization window.” Ansiaux et al. (22) subsequently found that the VEGF and basic fibroblast growth factor inhibitor thalidomide was able to increase tumor oxygenation by modifying tumor perfusion and interstitial pressure without radiosensitizing tumor cells, similar to the radiosensitization properties we have previously observed with the antiangiogenic peptide anginex (13).

Anginex is a designed peptide 33-mer and has been shown to induce anoikis in tumor activated endothelial cells (23). Recently, the molecular target of anginex was identified as galectin-1, which, during tumor angiogenesis, is crucial for activated endothelial cells to adhere to, and migrate on, the extracellular matrix (24). By weakly binding to plasma fibronectin (25), anginex is transported through the cardiovascular system to the tumor where the peptide strongly binds galectin-1 (K_d , 90 nmol/L), a glycan-binding protein that is highly up-regulated in tumor-activated endothelial cells (24). Anginex binding to galectin-1 disrupts tumor endothelial cell

adhesion and migration, inducing apoptosis and resulting in the inhibition of tumor angiogenesis. We recently showed that chronic or acute administration of anginex to tumor-bearing animals could significantly enhance the response to single or multiple doses of radiation therapy applied 1 or 2 days after the initiation of anginex treatment (13). We therefore sought to better understand the factors involved in the synergistic actions of anginex therapy and radiation-induced tumor growth delay.

Here, we investigated whether the non-growth factor pathway inhibitor anginex could normalize tumor vasculature and simultaneously elevate tumor oxygenation in three different tumor models, thereby supporting a mechanism of action for our previous results (13). As a reference therapy, we also tested the effects of Avastin on these end points in our models because this agent has already shown clinical potency and the suggestion of vessel normalization in human patients (5, 6). Our results show that both of these angiogenesis inhibition strategies can indeed transiently increase overall tumor oxygenation via vessel normalization. Moreover, we found that this increase in oxygenation enhances the effect of radiation therapy *in vivo* especially when radiation is applied at the peak of tumor oxygenation during therapy. These results may have immediate translational consequences for scheduling in the clinic because Avastin, in combination with chemotherapy and radiation, is already a Food and Drug Administration–approved protocol for treatment of several tumor types.

Materials and Methods

Mouse studies. Mice were purchased from the National Cancer Institute and allowed to acclimate to local conditions for at least 1 week. Animals were given water and standard chow *ad libitum* and were kept on a 12-h light/dark cycle. Experiments were approved by the University of Minnesota Research Animal Resources ethical committee. B16F10 murine melanoma cells (kindly provided by Dr. I.J. Fidler, Houston, TX), SCK murine mammary carcinoma (kindly provided by Dr. C. Song, Department of Therapeutic Radiology, University of Minnesota, Minneapolis, MN), and MA148 human ovarian carcinoma (kindly provided by Dr. S. Ramakrishnan, Department of Pharmacology, University of Minnesota, Minneapolis, MN) were cultured in RPMI 1640 with 10% bovine calf serum. A solution of 50 μ L with 2×10^5 of syngeneic B16F10 or SCK cells were injected s.c. in the right rear leg of male C57/BL6 or A/J mice, respectively. Female athymic nude mice (nu/nu, 5–6 weeks old) were s.c. inoculated with 2 million MA148 cells into the right flank.

When tumors reached a size of ~ 100 mm³ (40 days for MA148, 7 days for B16F10, and 5 days for SCK), treatment was initiated by administering anginex (10 mg/kg/d i.p. in the B16F10 and MA148 models and 20 mg/kg/d i.p. in the SCK model) or Avastin (10 mg/kg i.v. in a single injection) as previously described (13, 26). Avastin (bevacizumab) was purchased from Genentech through the University of Minnesota pharmacy and anginex was synthesized and purified as previously described (23).

Tumor oxygenation studies. Tumor partial pressure of oxygen (pO_2) was measured using an Eppendorf pO_2 histogram. A pO_2 electrode (300- μ m diameter, Eppendorf) was inserted by hand into tumors through small incisions made in the skin on the distal side of the tumor. The electrode, which was advanced into the tumor via computer control, measured pO_2 along the track. For this procedure, the electrode was advanced by 0.4-mm forward steps and then withdrawn by 0.3 mm to reduce compression pressure before recording the pO_2 value (13). The pO_2 values reported are the result of 120 to 700 individual readings derived from three to seven mice per group per day, with four tracks per mouse and 10 values per track.

Immunohistochemistry for tumor vessel density and pericyte involvement. Similar size tumors were either fixed in 10% formalin or were embedded in tissue freezing medium (Miles, Inc.) and snap frozen in liquid nitrogen. Formalin-fixed tumors embedded in paraffin or frozen tumors were cut into 5- μ m sections. After rehydration and antigen retrieval, the slides were stained for either vessel density (CD34; PharMingen) or pericytes (α -smooth muscle actin; PharMingen) developed with 3,3'-diaminobenzidine and lightly counterstained with hematoxylin. Preparation and procedures for the frozen tumor sections were done as described earlier (27). Briefly, sections were incubated in a 1:50 dilution with phycoerythrin-conjugated monoclonal antibody to mouse CD31 (platelet/endothelial cell adhesion molecule 1; PharMingen) or a FITC-conjugated monoclonal anti- α -smooth muscle actin antibody (Sigma Chemical) to stain for microvessel density or pericytes, respectively.

Immunohistochemical visualization of tumor hypoxia. An i.p. injection of 60 mg/kg pimonidazole was given to each mouse. Pimonida-

zole, a substituted 2-nitroimidazole with a molecular weight of 290.7, is preferentially reduced in hypoxic viable cells and forms irreversible protein adducts, which have been optimized for detection with immunohistochemistry. At 3 h postinjection, the mice were sacrificed, and the tumor was dissected and immediately either fixed in 10% formalin or snap frozen. Following sectioning of the tumor tissue, a FITC-conjugated monoclonal antibody against protein adducts of pimonidazole was added (hypoxyprobe-1 Mab1; Chemicon International). Images of the sections were acquired on Olympus BX-60 microscope at $\times 200$ magnification, then digitally analyzed and differentially quantified by morphometric analysis (28).

Radiation-induced tumor growth delay assays. In all three models, tumors were locally irradiated with 5 Gy using a Philips 250-kV X-ray machine at a dose rate of 1.4 Gy/min. The body was shielded with lead, and only the tumor and foot were exposed to the X-ray beam. Tumor volumes were measured using a caliper (Scienceware) and were calculated according to the equation $(a^2 \times b) / 2$, where a is the width

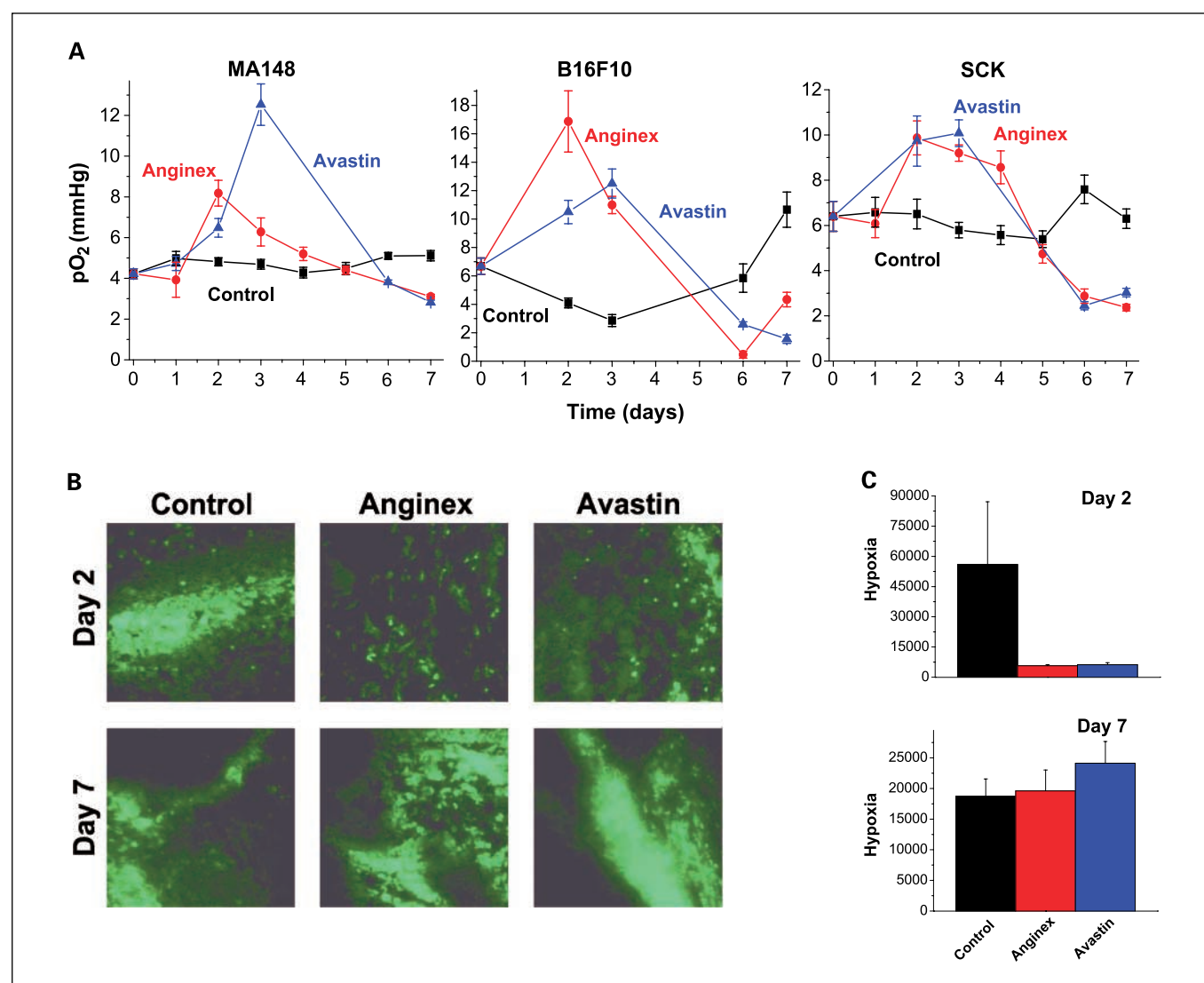


Fig. 1. The effect of anginex and Avastin (bevacizumab) on global tumor pO_2 over time. **A**, global tumor pO_2 is transiently increased by anginex and Avastin in MA148, B16F10, and SCK tumors as measured by Eppendorf pO_2 histogram. \blacksquare -, control; \bullet -, anginex; \blacktriangle -, Avastin. Points, average median pO_2 value derived from, on average, 10 values per track, 4 tracks per mouse and 3 to 7 mice per treatment group per day ($n = 120-700$); bars, SE. **B**, typical pimonidazole stainings of control, anginex, and Avastin treatment of SCK tumors on days 2 and 7. Representative images of the means for the amount of staining across each section. Original magnification, $\times 200$; bar, 50 μ m. **C**, quantification of pimonidazole stainings of SCK tumors on days 2 and 7 by morphometric analysis. Following binarization of images, hypoxia was estimated by scoring the total number of white pixels per field. Columns, mean black pixel count per image; bars, SE.

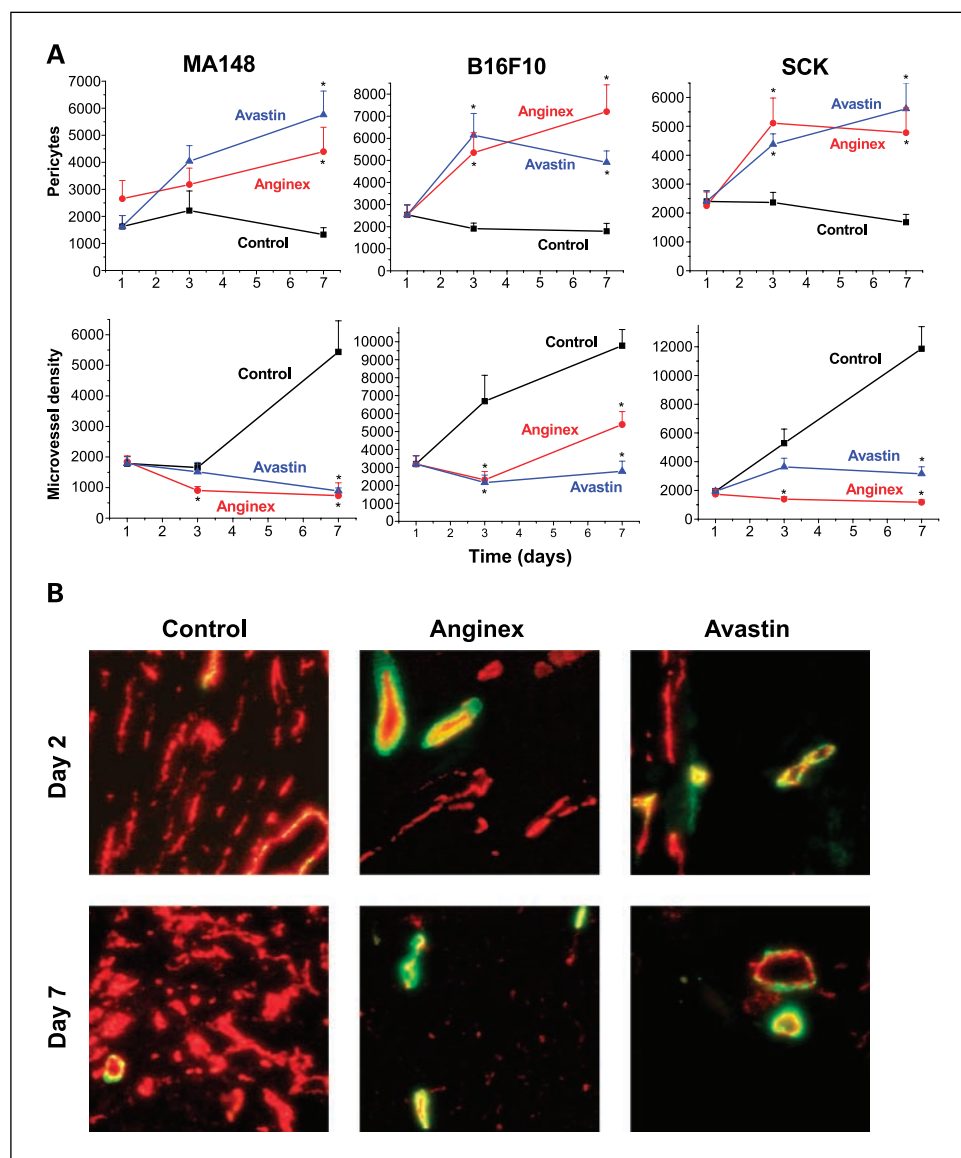


Fig. 2. Histologic analysis of pericytes and microvessel density after treatment with anginex and Avastin. *A*, quantification of immunohistochemical staining for pericytes and microvessel density in MA148, B16F10, and SCK tumors by morphometric analysis. *, $P < 0.01$, experimental group compared with control (Student's *t* test). *B*, typical colocalization staining of pericytes (green) and microvessel density (red) for control, anginex-treated, and Avastin-treated SCK tumors on days 2 and 7. Representative images of the means for the amount of staining. Original magnification, $\times 200$; bar, 50 μm .

and *b* is the length of the tumor. As an indirect measurement of general toxicity, body weights of mice were monitored using a digital balance (Ohaus).

Synergy determination. To determine the degree to which the combination of anginex or Avastin and radiation had synergistic effects on tumor growth delay, the following formula was applied: (observed growth delay from combination treatment) / {(tumor growth delay from treatment 1) + (tumor growth delay from treatment 2)} (13, 26). A ratio >1 indicates a synergistic (greater than additive) effect. Growth delay was calculated by subtracting the average time for control tumors to grow 4-fold in volume from the time required for treated tumors to increase in volume by the same amount from the day of radiation.

In vitro cell clonogenic assay. Human umbilical vein endothelial cells, obtained from the Ob/Gyn Department at the University of Minnesota, or B16F10 cells were cultured in RPMI 1640 with 20% or 10% bovine calf serum, respectively. Cells in exponential growth phase were trypsinized, washed, counted, and seeded into 25 cm^2 tissue culture flasks in duplicate for all conditions. The flasks were incubated overnight at 37°C, exposed to anginex (20 μM) for 4 h and then irradiated (5 Gy) or vice versa, rinsed once with normal medium, and incubated with fresh medium for 7 to 10 days in a 5% $\text{CO}_2/95\%$ air,

37°C incubator. The resulting colonies were stained with crystal violet in methanol/acetic acid (10:1) and counted by hand, as described earlier (13).

Results and Discussion

Thus far, studies on vessel normalization have only focused on compounds that inhibit growth factor pathways (i.e., VEGFR2 and thalidomide), with tumor oxygenation being measured locally and indirectly by immunohistochemistry or by electron paramagnetic resonance oximetry (using charcoal as an oxygen-sensitive probe; refs. 21, 22). In this report, overall daily tumor oxygenation levels in mice were measured directly and in real time using an Eppendorf $p\text{O}_2$ histogram. Our results support previously reported changes in tumor oxygenation measured indirectly (21, 22). The Eppendorf machine used here allows measurement of tumor oxygenation throughout the tumor using multiple tracks and numerous readings per track to accumulate up to 70 values per tumor, depending on

tumor size. Treatment with anginex resulted in an increase in overall tumor oxygenation up to day 4 of treatment (compared with vehicle-treated mice) in all three tumor models examined: xenograft human ovarian carcinoma MA148, murine melanoma B16F10, and murine breast carcinoma SCK (Fig. 1A). After day 4, tumor oxygenation decreased to levels below those in vehicle-treated mice. Pimonidazole distribution analysis subsequently confirmed these differences in tumor oxygenation levels (Fig. 1B and C). This suggests that oxygen elevation in tumors may be a general phenomenon induced by any angiogenesis inhibitor and not only by those targeting a growth factor-mediated pathway. It is also interesting to note that this "tumor oxygenation window" occurred in all three tumor models that vary in origin and growth rate. Lastly, our results agree with the time dependence in angiogenesis inhibitor-induced tumor oxygenation reported in other studies (13, 21, 22).

For comparison, we further investigated whether Avastin transiently elevates tumor oxygenation in the same tumor models. Capturing free VEGF by Avastin mimics the binding of the soluble Flt-1 VEGF receptor, which is the natural inhibition mechanism for the bioavailability of VEGF. This recombinant humanized monoclonal antibody is composed of the consensus human immunoglobulin G1 framework regions and the antigen-binding regions from the murine IgG1 anti-human VEGF monoclonal antibody A.4.6.1 (29). The antibody is cross-reactive with other species, although with a lower affinity compared with human VEGF (30). Interspecies biological effect of the antibody has already been shown via wound healing inhibition in a rabbit dermal wound model (31), as well as by tumor growth inhibition of human tumors in murine xenografts (32). Here, we show that Avastin also transiently elevates tumor oxygenation in all three tumor models, also up to day 4 as noted above with anginex. The decrease in tumor oxygenation after the 4th day was also found with Avastin

(Fig. 1A), which was confirmed by the distribution of pimonidazole (Fig. 1B and C). Interestingly, the kinetics of the tumor oxygenation window were once again similar among the three tumor models and consistent with previous studies using other agents (21, 22). Collectively, our results and those of others indicate that these effects from different angiogenesis inhibitors against existing tumor vasculature are generally consistent and reproducible. Whether or not this phenomenon reoccurs on subsequent rounds of therapy, an important clinical question, remains to be determined.

The next question we addressed is whether "vessel normalization" is the mechanism by which tumor oxygenation is transiently increased and then deteriorates during anginex or Avastin therapy. Immunohistochemical analysis indicated that there was a time-dependent increase in the amount of pericytes in tumors treated with either anginex or Avastin (Fig. 2A). This trend was observed in all three tumor models, as quantified by morphometric analysis (28). Microvessel density was also reduced using either antiangiogenesis strategy (Fig. 2A). Apparently, tumor vessels that already had pericyte coverage, or those that could rapidly recruit it, were able to survive angiostatic treatment. In addition, the morphology of the remaining vessels seemed to be larger, indicating that smaller "immature" vessels were preferentially eliminated. Hence, sustained exposure to anginex or Avastin may have increased the actual and relative amount of pericyte coverage in tumor vessels over time (Fig. 2B).

The therapeutic relevance of anginex- or Avastin-induced increases in tumor oxygenation to radiation treatment was investigated by varying the schedules of antiangiogenic and radiation therapies (Table 1; Fig. 3). Body weights of mice were monitored as an indirect measurement of general toxicity. Animals treated with anginex or Avastin (alone or in combination with radiation) showed no signs of toxicity as assessed by unaltered behavior, weight gain during experiments,

Table 1. The effects on tumor growth delay by multiple treatment schedules of anginex, Avastin, and radiation

	MA148			B16F10			SCK		
	Quadruple time (d)*	Growth delay (d) [†]	S [‡]	Quadruple time (d)*	Growth delay (d) [†]	S [‡]	Double time (d) [§]	Growth delay (d) [†]	S [‡]
Control	23.0 ± 2.1			4.0 ± 0.4			2.2 ± 0.3		
Rt ₂	28.0 ± 0.0	5.0		5.1 ± 0.5	1.1		3.0 ± 0.3	0.8	
Ax ₀₊₁	23.8 ± 4.2	0.8		4.6 ± 0.6	0.6		2.0 ± 0.3	0	
Rt ₂ Ax ₂₊₃	29.8 ± 3.6	6.8	1.2	5.6 ± 0.5	1.6	0.9	3.2 ± 0.4	1.0	1.3
Ax ₀₊₁ Rt ₂ [¶]	∞	∞		7.5 ± 0.4	3.5	2.1	3.5 ± 0.3	1.3	1.6
Av ₀	nd	nd		3.6 ± 0.4	0		2.3 ± 0.2	0.1	
Rt ₂ Av ₂ [§]	nd	nd		5.9 ± 0.3	1.9	1.7	2.6 ± 0.3	0.4	0.4
Av ₀ Rt ₂ [¶]	nd	nd		7.3 ± 0.4	3.3	3.0	3.3 ± 0.3	1.1	1.2

NOTE: Data are presented as mean ± SE (*n* = 5-8 per group).

Abbreviations: Rt, radiation (5 Gy); Ax, anginex (10 mg/kg for MA148 and B16F10 or 20 mg/kg for SCK i.p., 2 d); Av, Avastin (10 mg/kg i.v., once); nd, not determined; ∞, indefinite due to tumor regression. Subscripts refer to the days the treatments were given.

*The time it took to quadruple in tumor volume as calculated for each individual mouse starting on the day radiation was initiated (day 2; 5 Gy).

[†]Growth delay is defined as the delay in quadruple time as compared with vehicle treated animals.

[‡]Synergy ratio.

[§]The time it took to double in tumor volume as calculated for each individual mouse starting on the day radiation (5 Gy) was initiated (day 2).

Time to quadruple in volume was not achieved due to early deaths or sacrificing of mice in moribund state.

^{||}Angiostatic treatment was given 2 d postradiation.

[¶]Angiostatic treatment was given 2 d before radiation.

and macroscopic and microscopic morphology of internal organs on autopsy. This was in line with previous observations (13, 26, 27, 33).

In one therapeutic approach, tumor-bearing mice were treated with anginex either for 2 days before a single tumor irradiation at 5 Gy or for 2 days after radiation treatment. In the MA148 model, for example, tumors quadrupled in size in 23.0 ± 2.1 or 23.8 ± 4.2 days in mice treated with vehicle or anginex (2 daily i.p. injections of 10 mg/kg), respectively. Radiation treatment (5 Gy) alone delayed quadrupling time by 5.0 days compared with untreated mice. However, when the same radiation dose was administered 1 day after 2 days of anginex treatment, tumors initially regressed in size and then remained dormant (Table 1; Fig. 3). However, when anginex treatment followed radiation, this effect was not observed, yet tumor growth (quadrupling time) was delayed by 6.8 days compared with control. Clearly, the greater effect on tumor growth occurred when anginex was administered before radiation treatment. Similar results were also found here using anginex in the B16F10 melanoma and SCK breast carcinoma (Table 1).

In addition, Avastin induced nearly identical effects on the tumor response to radiation in the B16F10 and SCK tumor models (Table 1). For example, in the B16F10 model, tumors quadrupled in size when treated with vehicle (4.0 ± 0.4 days) or with Avastin (3.6 ± 0.4 days), whereas radiation treatment alone delayed quadrupling time by 1.1 days. When Avastin was administered before radiation, however, tumors quadrupled in size in 7.3 ± 0.4 days, a delay of 3.3 days compared with control (Table 1). This effect was synergistic (synergy ratio, 3.0; Table 1). On the other hand, when Avastin was administered after radiation, a quadrupling time delay of only 1.9 days was observed. Whereas this effect was also found to be synergistic

Table 2. The effects on tumor growth delay by fractionated radiation (2×5 Gy) on two different time intervals combined with anginex

B16F10	Quadruple time (d)*	Growth delay (d) [†]	S [‡]
Control	3.3 ± 0.2		
Ax ₀₋₂	3.6 ± 0.6	0.3	
Rt ₂₊₃	5.9 ± 0.7	2.6	
Ax ₀₋₂ Rt ₂₊₃ [§]	13.5 ± 2.9	10.2	3.5
Ax ₀₋₅	3.0 ± 0.5	0	
Rt ₅₊₆	6.3 ± 0.5	3.0	
Ax ₀₋₅ Rt ₅₊₆ [§]	7.9 ± 0.7	4.6	1.5

NOTE: Data are presented as mean \pm SE ($n = 6-8$ per group). Abbreviations: Rt, radiation (2×5 Gy); Ax, anginex (10 mg/kg i.p., 3 d). Subscripts refer to the days the treatments were given, respectively.

*The time it took to quadruple in tumor volume as calculated for each individual mouse starting on the day radiation treatment was initiated (day 2 or day 5).

[†]Growth delay is defined as the delay in quadruple time as compared with vehicle-treated animals.

[‡]Synergy ratio.

[§]Angiostatic treatment was given 3 or 6 d before radiation.

(synergy ratio, 1.7; Table 1), it was clearly less than Avastin treatment before radiation.

To further understand the relevance of the measured tumor oxygenation changes induced by anginex on radiation response, we also compared the therapeutic potential of administering anginex for 3 and 6 days before fractionated radiation. We hypothesized that the radiation response is greatest when radiation is administered during the oxygenation window (days

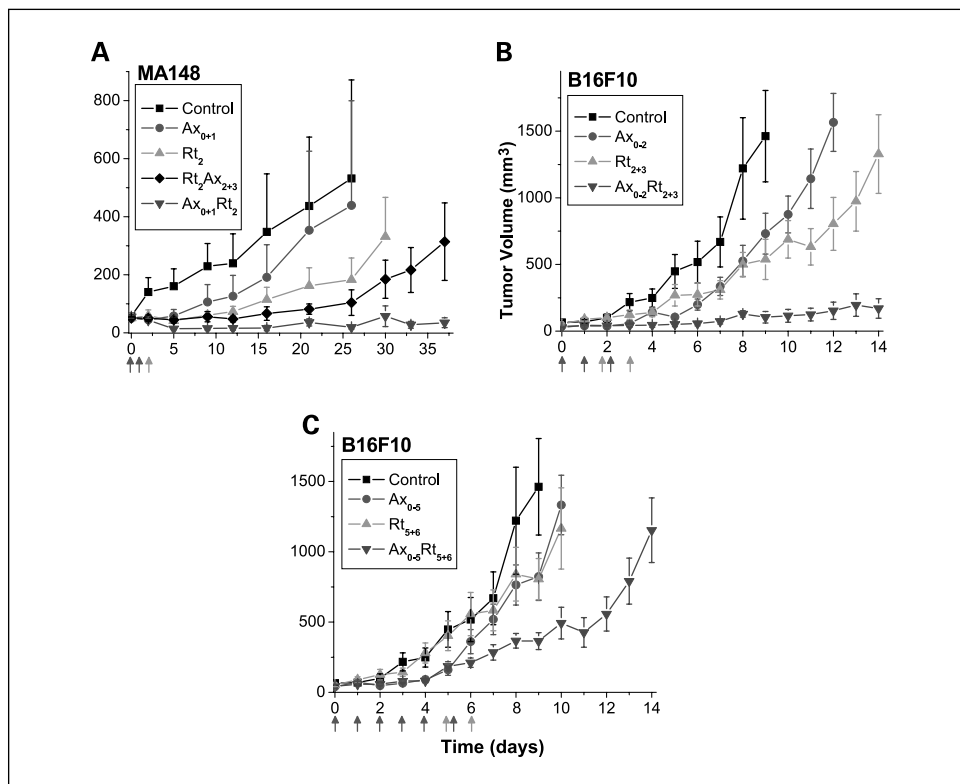
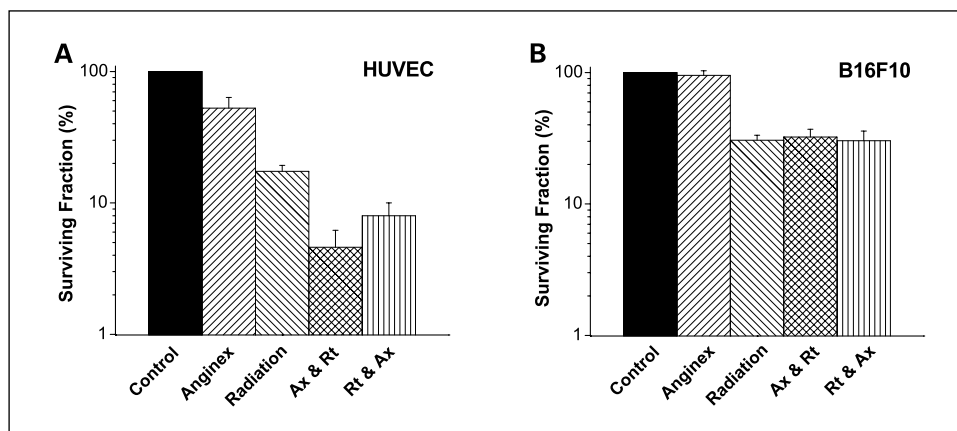


Fig. 3. Radiation treatment enhancement by rational scheduling of angiogenesis inhibitors. *A*, MA148 tumor volumes after anginex, radiation, or combination treatment. Tumor-bearing animals were treated with control (■-), anginex (●-; i.p. injections of 10 mg/kg Ax on days 0 and 1), radiation (▲-; 5 Gy, day 2), RtAx combination (◆-; 5 Gy on day 2 followed by Ax on days 2 and 3), and AxRt combination (▼-; Ax on days 0 and 1 followed by 5 Gy on day 2). *B*, B16F10 tumor volumes after anginex, radiation, or combination treatment. Tumor-bearing animals were treated with control (■-), anginex (●-; i.p. injections of 10 mg/kg Ax on days 0-2), radiation (▲-; 5 Gy, days 2 and 3), and AxRt combination (▼-; Ax on days 0-2 followed by 5 Gy on days 2 and 3). *C*, B16F10 tumor volumes after anginex, radiation, or combination treatment. Tumor-bearing animals were treated with control (■-), anginex (●-; i.p. injections of 10 mg/kg Ax on days 0-5), radiation (▲-; 5 Gy, days 5 and 6), and AxRt combination (▼-; Ax on days 0-5 followed by 5 Gy on days 5 and 6). Points, mean tumor volume ($n = 5-8$ animals per group); bars, SE.

Fig. 4. Anginex specifically targets and enhances the antiproliferative activity of radiation on endothelial cells. *A*, anginex radiosensitizes endothelial cells. Clonogenicity of human umbilical vein endothelial cells (*HUVEC*) is reduced to 50% by anginex exposure (20 $\mu\text{mol/L}$ for 4 h) or to 17% by 5-Gy radiation treatment. Combining anginex before radiation caused an enhanced decrease in clonogenicity (4.6% $P < 0.006$) compared with either monotherapy alone. *B*, anginex has no effect on colony formation of B16F10 cells. The survival fraction was reduced by 70% by exposure to 5 Gy alone, but was not further decreased when anginex (20 $\mu\text{mol/L}$ for 4 h) was combined before or after radiation.



2 and 3), as opposed to other times. To test this hypothesis, we treated B16F10 tumor-bearing mice either with anginex for 3 days (days 0-2) followed by radiation on days 2 and 3, or with anginex for 6 days (days 0-5) followed by radiation on days 5 and 6. In mice treated with vehicle or anginex, tumors quadrupled in size in 3.3 ± 0.2 or 3.6 ± 0.6 days, respectively. Radiation treatment (2×5 Gy on days 2 and 3) alone delayed quadrupling time by 2.6 days. However, when the same fractionated radiation dose was initiated 1 day after 2 days of anginex treatment, the quadrupling time increased to 13.5 ± 2.9 days, yielding a growth delay of 10.2 days compared with vehicle-treated mice. This effect on tumor growth was synergistic (Table 2; Fig. 3). When anginex treatment was given for 5 days before initiating fractionated radiation treatment, tumor growth (quadrupling time) was delayed by 4.6 days, which was also found to be synergistic, albeit markedly less so than the effect on tumors irradiated within the oxygenation window.

Overall, we found that there was a supra-additive effect from anginex or Avastin treatment administered for short periods of time before radiation. Enhancement of the radiation response was less evident when the treatment period of the angiogenesis inhibitor was extended before radiation (Table 2; Fig. 3). Although we and others previously observed significant increases in tumor growth delay when antiangiogenics were administered before or during radiotherapy, the reason(s) for this were not clear.

Our results further show that anginex specifically targets and enhances antiproliferative activity of radiation on endothelial cells with negligible direct effects on tumor cells (Fig. 4). Anginex reduced endothelial cell colony formation to 50% but did not have an effect on B16F10 cells. On the other hand, radiation exposure alone reduced colony formation of endothelial cells to 17% and B16F10 cells to 30%. The combination of anginex and radiation resulted in enhanced effects only on endothelial cell survival, but not in B16F10 cells. Moreover,

giving anginex before radiation further decreased endothelial cell survival ($4.6 \pm 1.6\%$; $P < 0.006$) compared with anginex given postirradiation ($8.0 \pm 2.0\%$; Fig. 4). Therefore, the effects of anginex on endothelial cells seem to modify radiation-induced cell death by multiple mechanisms, including direct sensitization when applied before radiation and possibly perturbation of repair and survival signaling when applied after radiation, as previously suggested by others (10, 11).

In summary, mechanistically, anginex and other antiangiogenic agents are unable to directly sensitize tumor cells to radiation but do exhibit varying levels of radiosensitization of endothelial cells, leading to an improved radiation response *in vitro*. Furthermore, this and other studies indicate that tumor endothelial cell sensitization and increased tumor tissue oxygenation *in vivo* are integral to the mechanism of action at both the cellular and physiologic levels. This finding may be of immediate translational importance because in an ongoing phase I/II trial, patients with T_3 or T_4 rectal cancer are being given Avastin in combination with 5-fluorouracil and radiation. However, these patients are given Avastin roughly 2 weeks before radiation treatment or 5-fluorouracil chemotherapy (34). In view of our present results, Avastin normalization window appears within the first few days of treatment, similar to that found for thalidomide and VEGFR2 inhibitor (20, 22). After those first few days of antiangiogenic treatment, there is a progressive decrease (at least in these animal models) in tumor oxygenation, and this could compromise optimal effectiveness of radiation treatment or chemotherapy for patients waiting 2 weeks post-Avastin. Clearly, basic research and appropriately designed clinical studies continue to be worthwhile efforts to further optimize scheduling of combined antiangiogenic and radiation therapies.

Acknowledgments

We thank Colleen Forster for histology preparations.

References

- Griffioen AW, Molema G. Angiogenesis: potentials for pharmacologic intervention in the treatment of cancer, cardiovascular diseases, and chronic inflammation. *Pharmacol Rev* 2000;52:237–68.
- Ferrara N, Davis-Smyth T. The biology of vascular endothelial growth factor. *Endocr Rev* 1997;18:4–25.
- Lordick F, Geinitz H, Theisen J, Sender A, Sarbia M. Increased risk of ischemic bowel complications during treatment with bevacizumab after pelvic irradiation: report of three cases. *Int J Radiat Oncol Biol Phys* 2006;64:1295–8.
- Griffin RJ, Molema G, Dings RP. Angiogenesis treatment, new concepts on the horizon. *Angiogenesis* 2006;9:67–72.
- Willett CG, Boucher Y, di Tomaso E, et al. Direct evidence that the VEGF-specific antibody bevacizumab has antivascular effects in human rectal cancer. *Nat Med* 2004;10:145–7.
- Hurwitz H, Fehrenbacher L, Novotny W, et al. Bevacizumab plus irinotecan, fluorouracil, and leucovorin for metastatic colorectal cancer. *N Engl J Med* 2004;350:2335–42.
- Miller KD, Chap LI, Holmes FA, et al. Randomized phase III trial of capecitabine compared with

- bevacizumab plus capecitabine in patients with previously treated metastatic breast cancer. *J Clin Oncol* 2005;23:792–9.
8. Kerbel RS, Yu J, Tran J, et al. Possible mechanisms of acquired resistance to anti-angiogenic drugs: implications for the use of combination therapy approaches. *Cancer Metastasis Rev* 2001;20:79–86.
 9. Hanna NN, Seetharam S, Mauceri HJ, et al. Antitumor interaction of short-course endostatin and ionizing radiation. *Cancer J* 2000;6:287–93.
 10. Gorski DH, Mauceri HJ, Salloum RM, et al. Potentiation of the antitumor effect of ionizing radiation by brief concomitant exposures to angiostatin. *Cancer Res* 1998;58:5686–9.
 11. Mauceri HJ, Hanna NN, Beckett MA, et al. Combined effects of angiostatin and ionizing radiation in antitumor therapy. *Nature* 1998;394:287–91.
 12. Griffin RJ, Williams BW, Wild R, Cherrington JM, Park H, Song CW. Simultaneous inhibition of the receptor kinase activity of vascular endothelial, fibroblast, and platelet-derived growth factors suppresses tumor growth and enhances tumor radiation response. *Cancer Res* 2002;62:1702–6.
 13. Dings RP, Williams BW, Song CW, Griffioen AW, Mayo KH, Griffin RJ. Anginex synergizes with radiation therapy to inhibit tumor growth by radiosensitizing endothelial cells. *Int J Cancer* 2005;115:312–9.
 14. Citrin D, Menard C, Camphausen K. Combining radiotherapy and angiogenesis inhibitors: clinical trial design. *Int J Radiat Oncol Biol Phys* 2006;64:15–25.
 15. Carter SK. Clinical strategy for the development of angiogenesis inhibitors. *Oncologist* 2000;5 Suppl 1: 51–4.
 16. Fogarty M. Learning from angiogenesis trial failures. *The Scientist* 2002;16:33–5.
 17. Gorski DH, Beckett MA, Jaskowiak NT, et al. Blockage of the vascular endothelial growth factor stress response increases the antitumor effects of ionizing radiation. *Cancer Res* 1999;59:3374–8.
 18. Abdollahi A, Lipson KE, Sckell A, et al. Combined therapy with direct and indirect angiogenesis inhibition results in enhanced antiangiogenic and antitumor effects. *Cancer Res* 2003;63:8890–8.
 19. Hess C, Vuong V, Hegyi I, et al. Effect of VEGF receptor inhibitor PTK787/ZK222584 [correction of ZK222548] combined with ionizing radiation on endothelial cells and tumour growth. *Br J Cancer* 2001; 85:2010–6.
 20. Jain RK. Normalizing tumor vasculature with anti-angiogenic therapy: a new paradigm for combination therapy. *Nat Med* 2001;7:987–9.
 21. Winkler F, Kozin SV, Tong RT, et al. Kinetics of vascular normalization by VEGFR2 blockade governs brain tumor response to radiation: role of oxygenation, angiopoietin-1, and matrix metalloproteinases. *Cancer Cell* 2004;6:553–63.
 22. Ansiaux R, Baudelet C, Jordan BF, et al. Thalidomide radiosensitizes tumors through early changes in the tumor microenvironment. *Clin Cancer Res* 2005; 11:743–50.
 23. Griffioen AW, van der Schaft DW, Barendsz-Janson AF, et al. Anginex, a designed peptide that inhibits angiogenesis. *Biochem J* 2001;354:233–42.
 24. Thijssen VL, Postel R, Brandwijk RJ, et al. Galectin-1 is essential in tumor angiogenesis and is a target for antiangiogenesis therapy. *Proc Natl Acad Sci U S A* 2006;103:15975–80.
 25. Akerman ME, Pilch J, Peters D, Ruoslahti E. Angiostatic peptides use plasma fibronectin to home to angiogenic vasculature. *Proc Natl Acad Sci U S A* 2005; 102:2040–5.
 26. Dings RP, Yokoyama Y, Ramakrishnan S, Griffioen AW, Mayo KH. The designed angiostatic peptide anginex synergistically improves chemotherapy and anti-angiogenesis therapy with angiostatin. *Cancer Res* 2003;63:382–5.
 27. Dings RP, Chen X, Hellebrekers DM, et al. Design of nonpeptidic topomimetics of antiangiogenic proteins with antitumor activities. *J Natl Cancer Inst* 2006;98: 932–6.
 28. Wild R, Ramakrishnan S, Sedgewick J, Griffioen AW. Quantitative assessment of angiogenesis and tumor vessel architecture by computer-assisted digital image analysis: effects of VEGF-toxin conjugate on tumor microvessel density. *Microvasc Res* 2000;59: 368–76.
 29. Presta LG, Chen H, O'Connor SJ, et al. Humanization of an anti-vascular endothelial growth factor monoclonal antibody for the therapy of solid tumors and other disorders. *Cancer Res* 1997;57:4593–9.
 30. van der Flier M, Coenjaerts FE, Mwinzi PN, et al. Antibody neutralization of vascular endothelial growth factor (VEGF) fails to attenuate vascular permeability and brain edema in experimental pneumococcal meningitis. *J Neuroimmunol* 2005;160:170–7.
 31. Leach W, Shopp G. Safety evaluation of bevacizumab in a rabbit dermal wound. South San Francisco (CA): Report Genentech; 1997.
 32. du Manoir JM, Francia G, Man S, et al. Strategies for delaying or treating *in vivo* acquired resistance to trastuzumab in human breast cancer xenografts. *Clin Cancer Res* 2006;12:904–16.
 33. Mayo KH, Dings RP, Flader C, et al. Design of a partial peptide mimetic of anginex with antiangiogenic and anticancer activity. *J Biol Chem* 2003;278: 45746–52.
 34. Willett CG, Boucher Y, Duda DG, et al. Surrogate markers for antiangiogenic therapy and dose-limiting toxicities for bevacizumab with radiation and chemotherapy: continued experience of a phase I trial in rectal cancer patients. *J Clin Oncol* 2005;23:8136–9.

Clinical Cancer Research

Scheduling of Radiation with Angiogenesis Inhibitors Anginex and Avastin Improves Therapeutic Outcome via Vessel Normalization

Ruud P.M. Dings, Melissa Loren, Hanke Heun, et al.

Clin Cancer Res 2007;13:3395-3402.

Updated version Access the most recent version of this article at:
<http://clincancerres.aacrjournals.org/content/13/11/3395>

Cited articles This article cites 33 articles, 15 of which you can access for free at:
<http://clincancerres.aacrjournals.org/content/13/11/3395.full#ref-list-1>

Citing articles This article has been cited by 25 HighWire-hosted articles. Access the articles at:
<http://clincancerres.aacrjournals.org/content/13/11/3395.full#related-urls>

E-mail alerts [Sign up to receive free email-alerts](#) related to this article or journal.

Reprints and Subscriptions To order reprints of this article or to subscribe to the journal, contact the AACR Publications Department at pubs@aacr.org.

Permissions To request permission to re-use all or part of this article, use this link
<http://clincancerres.aacrjournals.org/content/13/11/3395>.
Click on "Request Permissions" which will take you to the Copyright Clearance Center's (CCC) Rightslink site.